SUPPLEMENTAL MATERIAL

Supplementary Figures and Legends

Legends for Movies

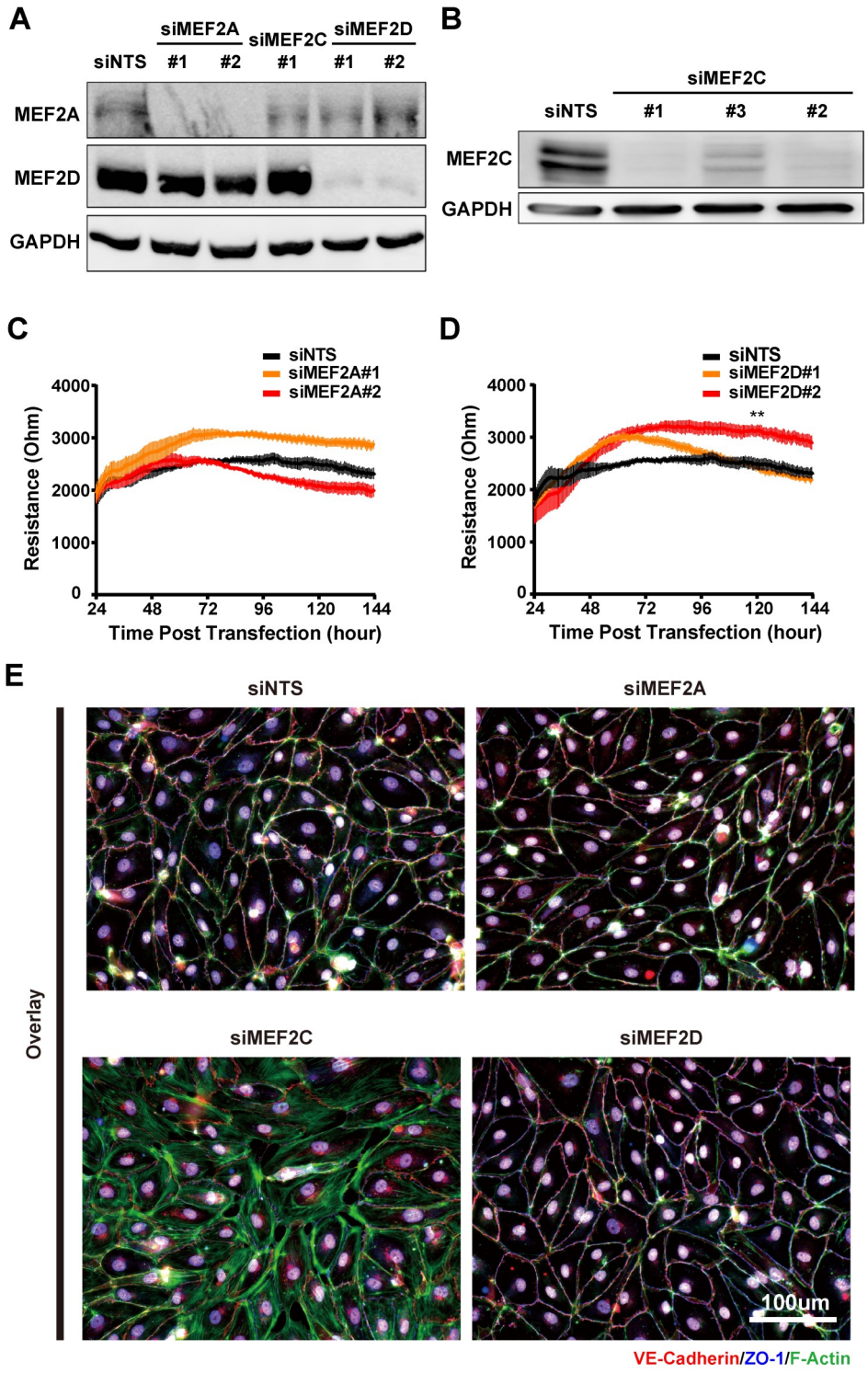

Supplemental Figure I. siRNA mediated knockdown of Mef2a or Mef2d in HDMECs does not cause increased permeability or actin stress fiber formation.

A, B, HDMECs were treated with non-targeting siRNA (siNTS) or with siRNA to MEF2A, MEF2D or MEF2C at the time of seeding. Monolayers were allowed to mature for 72 hours before harvest cell lysates for immunoblotting for MEF2A, MEF2D (**A**) or MEF2C (**B**) to assess knockdown efficiency for individual sets of siRNA oligonucleotides. **C, D,** HDMECs were treated with siNTS or with siRNAs to MEF2A (**C**) or MEF2D (**D**) at the time of seeding. Monolayers were allowed to mature for 24 hours before the electric resistance was measured by ECIS at 4000 Hz (n=3 independent experiments with duplicates). Results are presented as mean ± SEM, and the value recorded at 120 hours were used to perform one-way ANOVA analysis with Dunnett test to correct for multiple comparison (**, p<=0.01 when compared to siNTS). **E**, siRNA (siNTS, siMEF2A, siMEF2C or siMEF2D) transfected HDMECs were fixed 72 hrs post transfection and stained for VE-cadherin, ZO-1, and F-actin (phalloidin). Representative overlay images for each siRNAs (n=3 independent experiments).

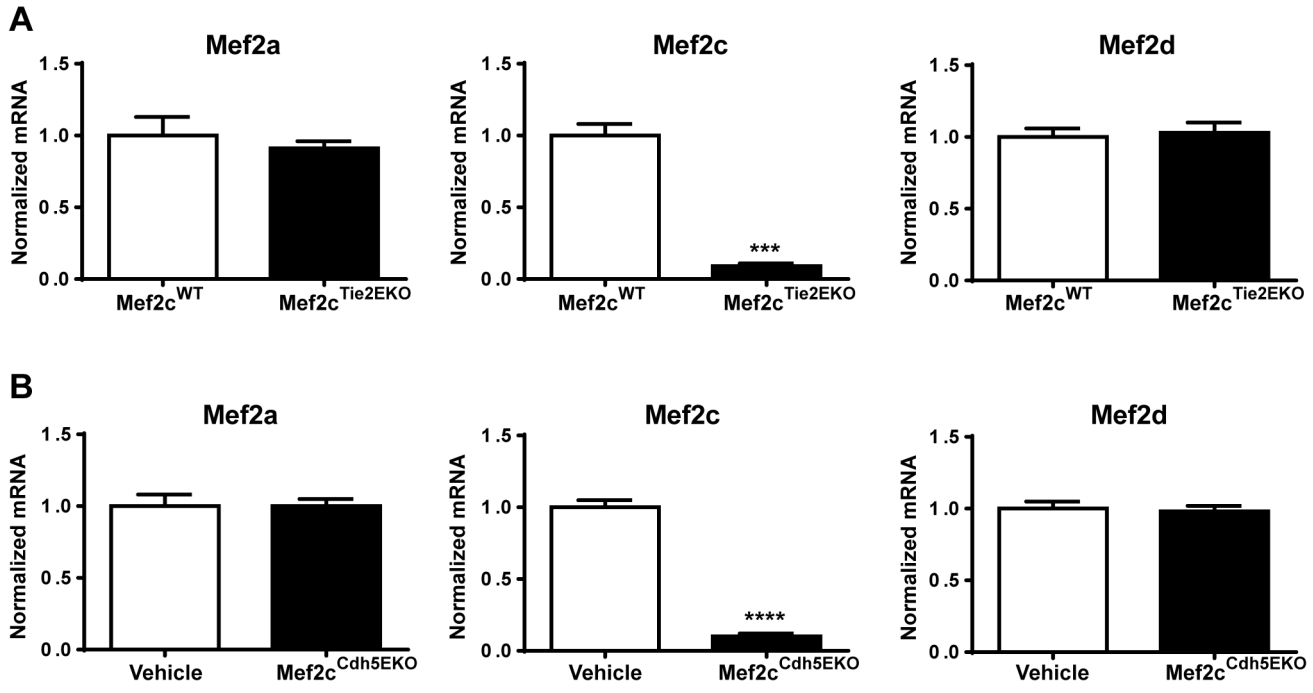

Supplemental Figure II. Endothelial-specific deletion of Mef2c does not alter Mef2a or Mef2d expression.

A, Endothelial RNA from thoracic aortas of Tie2-Cre mediated Mef2c deletion ($Mef2c^{Tie2EKO}$) and their littermate $Mef2c^{WT}$ controls were harvested at 20 weeks of age. **B**, Endothelial RNA from thoracic aorta of Cdh5-Cre^{ERT2} mediated deletion of Mef2c of 10 week-old mice after tamoxifen ($Mef2c^{Cdh5EKO}$) or vehicle injections. RNA was harvested 14 days after the first injection. Endothelial RNA was subsequently reverse-transcribed and assayed for Mef2a/c/d expression. Ct values were normalized to the housekeeping gene, Hprt. Results are presented as normalized mRNA to their respective controls. **A**, n=4 with materials from three mice pooled into each sample (***, p=0.0003 from student t-test). **B**, n=6 for Vehicle and n=7 for $Mef2c^{Cdh5EKO}$ with material from a single mouse in each sample (****, p<0.0001 from student t-test).

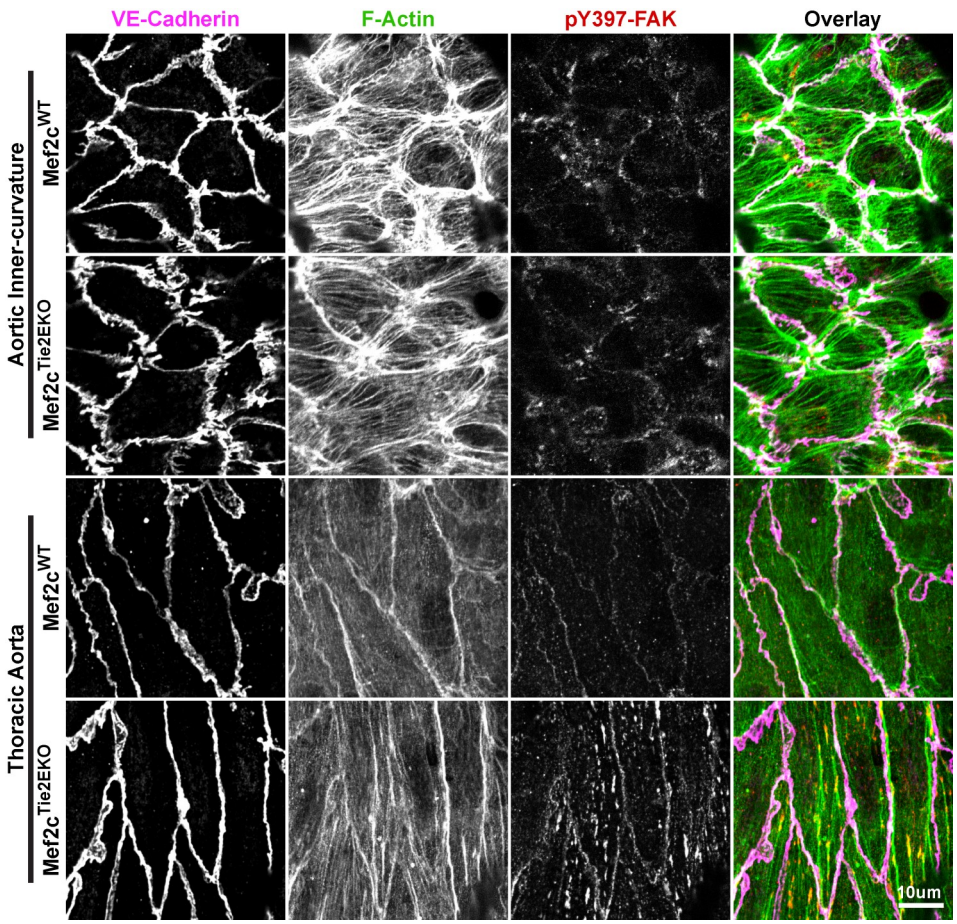

Supplemental Figure III. Endothelial Mef2c deletion increases FAK phosphorylation.

En face preparation and immunostaining were performed on thoracic aortas as described in methods. Aortic inner-curvature and thoracic aortas from $Mef2c^{Tie2EKO}$ and $Mef2c^{WT}$ control were labeled for immunofluorescence for VE-Cadherin, pY397-FAK, and F-actin (phalloidin). Representative confocal images are shown (n=3).

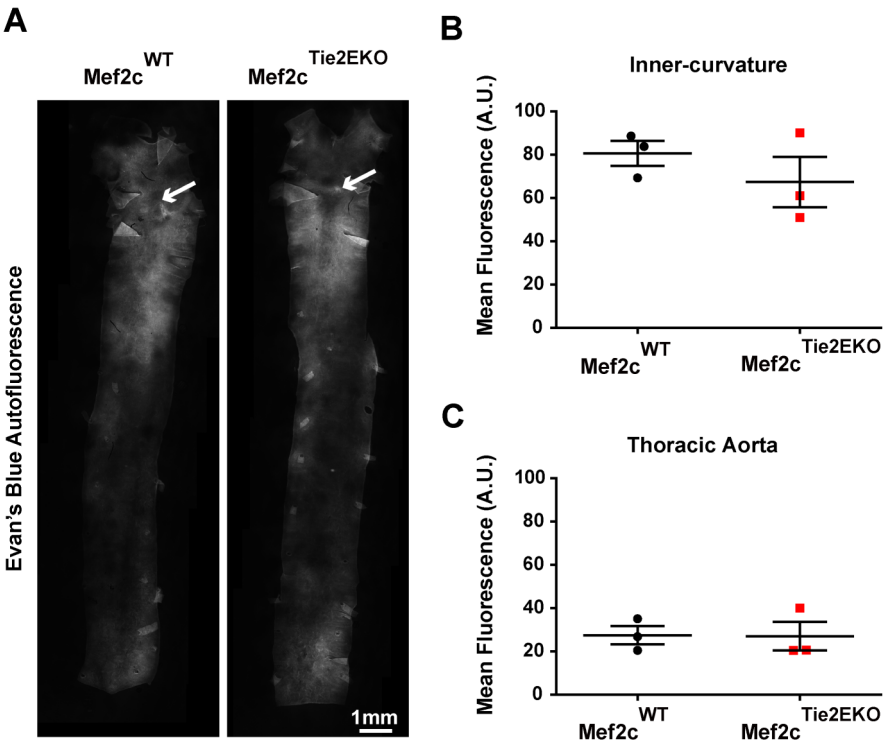

Supplemental Figure IV. Permeability of the aortic endothelium is unchanged by endothelial Mef2c deletion.

Mef2c^{Tie2EKO} and WT controls were injected with Evan's Blue and the aortas with thoracic and aortic arch were isolated after 30 minutes, fixed and imaged as described in methods. **A**, Representative image for the Evan's Blue autofluorescence detected in the far-red spectrum. **B, C**, Fluorescence quantification of Evan's Blue autofluorescence at the aortic inner-curvature (**B**) and thoracic aorta (**C**) (n=3). The inner curvature had higher Evan's blue signal than the thoracic aorta, indicative of higher albumin permeability, but there was no difference by student t-test between WT and Mef2c^{Tie2EKO}.

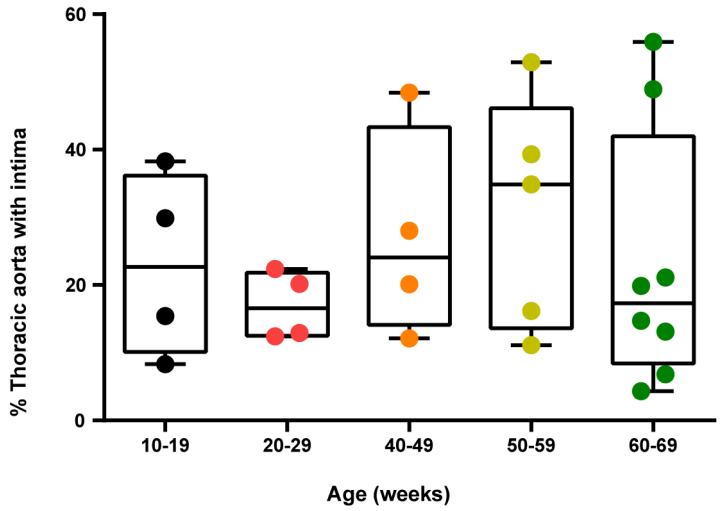

Supplemental Figure V. Distribution of intimal cell coverage by age of Mef2c^{Tie2EKO} mice revealed no change in coverage with increased age.

The relative area of F-actin-labeled intimal cells within aortas described in Figure 3F is plotted in bins by age to determine if the area increases with age. Area was quantified on 12-15 independent fields per thoracic aorta. Results are displayed as the percentage of area covered by intimal cells (10-19, n=4; 20-29, n=4; 40-49, n=4; 50-59, n=5; 60-69, n=8). All groups were compared against the 10-19 age group by one-way ANOVA with Dunnett test to correct for multiple comparisons; no significant differences between age groups were detected.

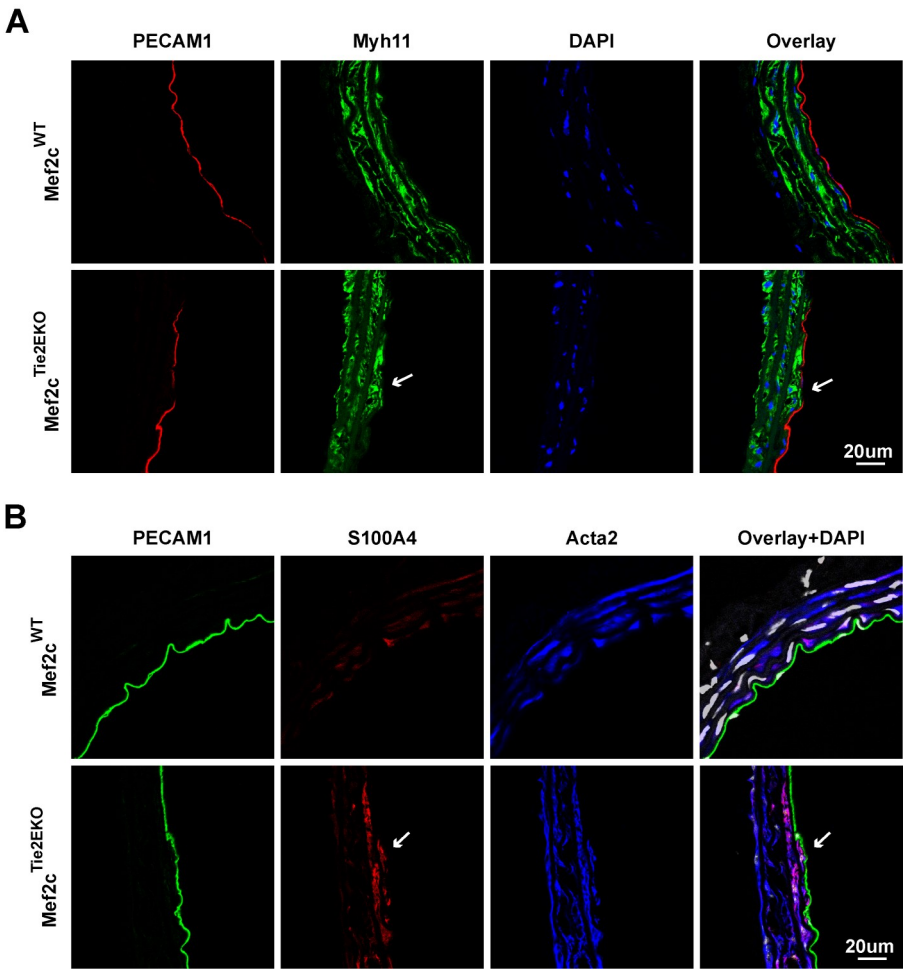

Supplemental Figure VI. Mef2c^{Tie2EKO} intimal cells in the thoracic aorta express smooth muscle markers.

Mef2c^{Tie2EKO} and control Mef2c^{WT} thoracic aortas were isolated, embedded in OCT and sectioned. They were then labeled for immunofluorescence with antibodies to Myh11 (**A**) or Acta2 and S100a4 (**B**) with co-labeling of endothelium (PECAM-1) and nuclei (DAPI), and imaged by confocal microscopy. The arrows indicate intimal cells expressing Myh11 (**A**) or S100a4 and Acta2 (**B**).

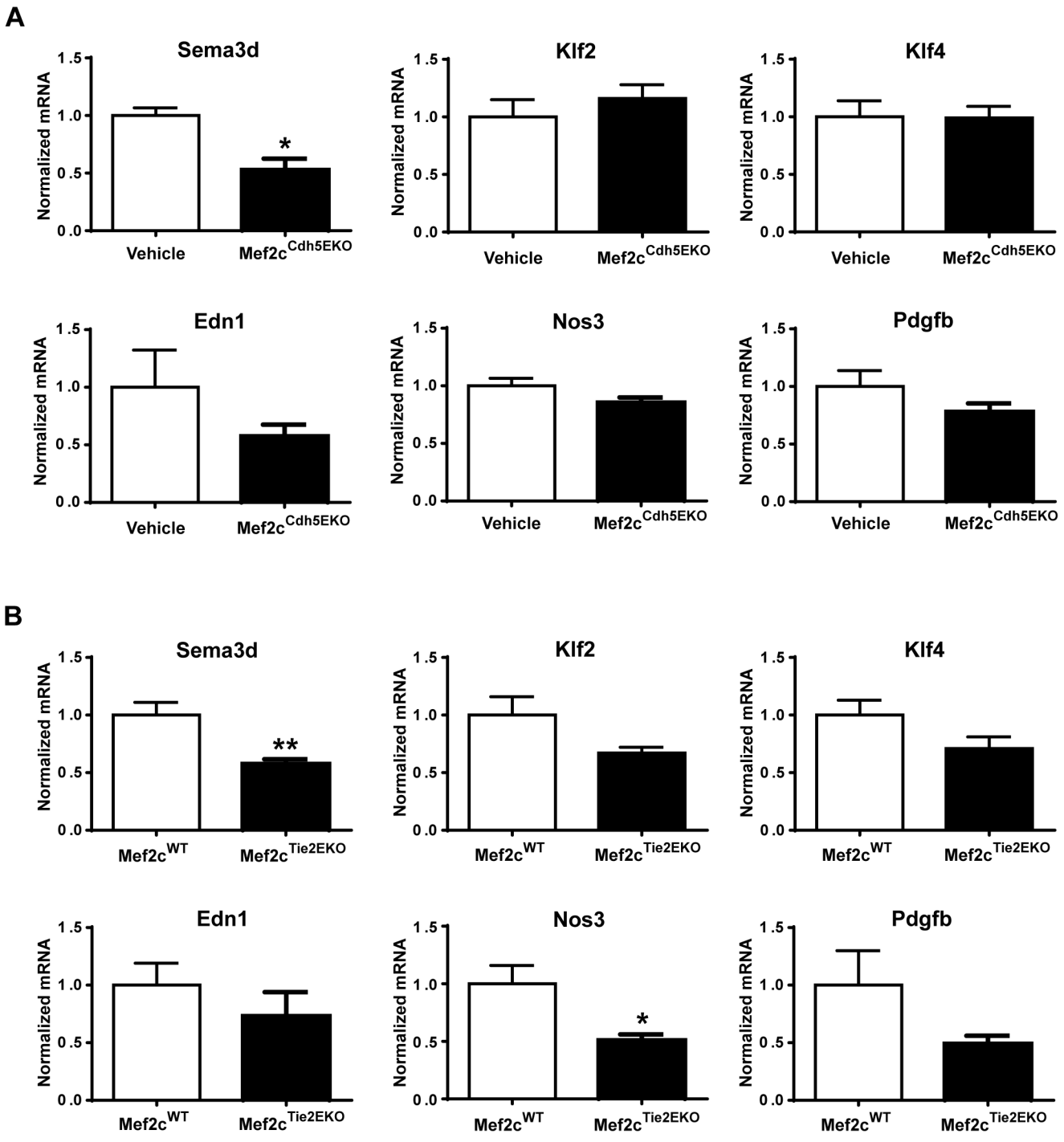

Supplemental Figure VII. Sema3d expression is reduced in Mef2c^{Cdh5EKO} and Mef2c^{Tie2EKO} aortic endothelium.

A, Endothelial RNA from 10 week-old Mef2c^{Cdh5EKO} or control (vehicle) thoracic aortas were isolated 14 days after the first of 5 daily tamoxifen or vehicle injections. Each sample was from a single aorta (n=5 for Mef2c^{Cdh5EKO} and vehicle control). **B**, Endothelial RNA from thoracic aortas of Mef2c^{Tie2EKO} and their littermate Mef2c^{WT} controls were harvested at 20 weeks of age. Each sample was pooled from three aortas (n=4 for Mef2c^{Tie2EKO} and Mef2c^{WT}). Endothelial RNA was subsequently reverse-transcribed and assayed for the indicated genes by quantitative PCR. Ct values were normalized to the housekeeping gene, Hprt. Results are presented as normalized mRNA to their respective controls. (*, $p<0.05$ and **, $p<0.01$ from student t-test).

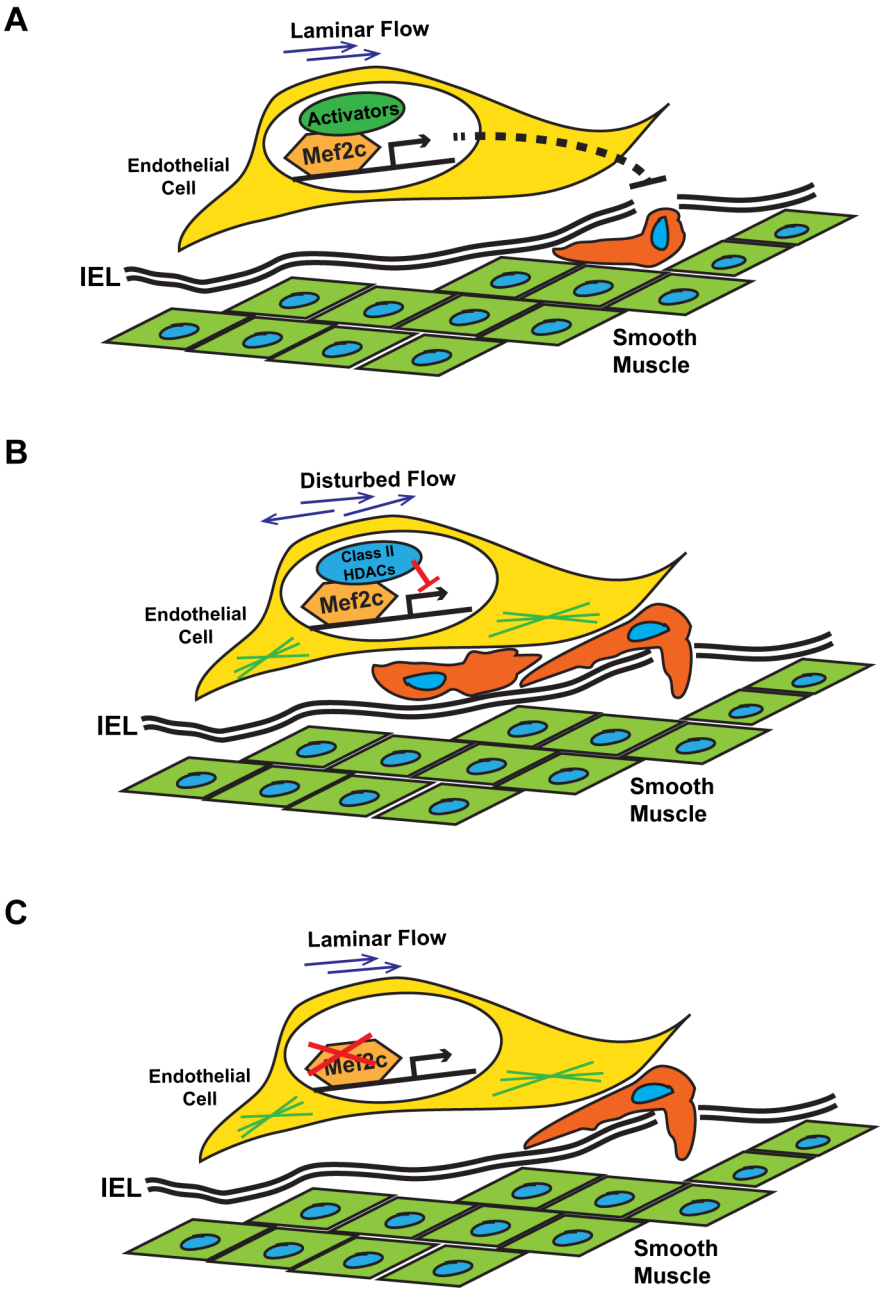

Supplemental Figure VIII. Model for Mef2c function in the endothelium.

A, We propose that Mef2c is a transcriptional activator through the actions of ERK5 and cytoplasmic localization of class II HDACs in LF regions leading to transcription of gene(s) in the endothelium that inhibit EC actin stress fiber formation and SM migration through fenestrations in the internal elastic lamina. **B**, Under DF, the Mef2s interact with class II HDACs to function as transcriptional repressors to repress transcription of gene(s) that inhibit EC actin stress fibers and SM migration thus allowing formation of ISM in regions such as the aortic inner curvature and branch points. **C**, When Mef2c is deleted, the endothelium in LF regions becomes more like DF regions with enhanced actin stress fibers and SM migration into the intima.

Movie 1. Representative migrating intimal smooth muscle cells from Mef2c^{Cdh5EKO}, Z-series.

Thoracic aortas of Mef2c^{Cdh5EKO} Rosa26^{Tomato} mice were processed for *en face* preparation and labeled for elastin (hydrazine), F-actin (phalloidin, not shown) and nuclei (DAPI). Representative confocal z-series is shown (n=7). Nuclei are shown in red; internal elastic lamina in cyan, and Cdh5-Cre-ER^{T2} driven tomato signal in green. Yellow arrows point to the fenestrations in the internal elastic lamina through which smooth muscle cells were migrating.

Movie 2. Representative migrating intimal smooth muscle cells from Mef2c^{Cdh5EKO}, 3D rendered.

Thoracic aortas of Mef2c^{Cdh5EKO} Rosa26^{Tomato} mice were processed for *en face* preparation and labeled for elastin (hydrazine), F-actin (phalloidin, not shown) and nuclei (DAPI). Confocal z-series were acquired and representative z-series were 3D rendered (Imaris, Bitplane) (n=7). Endothelial nuclei are shown in blue, migrating smooth muscle cell nuclei are in red, internal elastic lamina is in white/opaque, and medial smooth muscle nuclei are in purple. Yellow arrows point to the fenestration in the internal elastic lamina through which intimal smooth muscle cells were migrating.

Movie 3. Representative migrating intimal smooth muscle cells from carotid arteries of wild-type mice, Z-series.

Left carotid arteries of wild-type mice 10 days post-ligation were processed for *en face* preparation and labeled for elastin (hydrazine), F-actin (phalloidin, not shown) and nuclei (DAPI). Representative confocal z-series are shown (n=5). Nuclei are shown in red; internal elastic lamina in cyan. Yellow arrow points to a fenestration of the internal elastic lamina through which an intimal smooth muscle cells was migrating.

Movie 4. Representative migrating intimal smooth muscle cells from carotid arteries of wild-type mice, 3D rendered.

Left carotid arteries of wild-type mice 10 days post-ligation were processed for *en face* preparation and labeled for elastin (hydrazine), F-actin (phalloidin, not shown) and nuclei (DAPI). Confocal z-series were acquired and representative z-series were 3D rendered (Imaris, Bitplane) (n=5). Endothelial nuclei are shown in blue, migrating smooth muscle cell nucleus in red, internal elastic lamina in white/opaque, and medial smooth muscle nuclei in purple. Yellow arrow points to a fenestration of the internal elastic lamina through which intimal smooth muscle cell was migrating.